

# Quantum phonons and the charge density wave transition temperature: a dynamical mean field study

Stefan Blawid and Andrew J. Millis

*Center for Materials Theory*

*Department of Physics & Astronomy, Rutgers University*

*136 Frelinghuysen Road, Piscataway, NJ 08854*

(November 14, 2018)

We use the dynamical mean-field method to calculate the charge density wave transition temperature of the half-filled Holstein model as function of typical phonon frequency in the physically relevant adiabatic limit of phonon frequency  $\Omega$  much less than electron bandwidth  $t$ . Our work is the first systematic expansion of the charge density wave problem in  $\Omega/t$ . Quantum phonon effects are found to suppress  $T_{co}$  severely, in agreement with previous work on one dimensional models and numerical studies of the dynamical mean field model in the extreme antiadiabatic limit ( $\Omega \sim t$ ). We suggest that this is why there are very few CDW systems with mean-field transition temperatures much less than a typical phonon frequency.

71.45.Lr,71.10.-w,71.10.Fd,71.10.Hf

## I. INTRODUCTION

The present-day understanding of electron-lattice interactions in metals is based on the Migdal-Eliashberg (ME) theory<sup>1</sup>, which exploits the smallness of typical phonon frequencies,  $\Omega$ , and temperatures,  $T$ , relative to typical electronic energies,  $t$ . This theory may be regarded as an expansion in powers of the adiabatic parameter  $\gamma = \max(\Omega, T)/t$ , in which only the leading non-trivial term is retained. In many cases the leading term is of order  $\gamma^0$  and thus within ME theory most quantities of physical interest are independent of ion mass. A notable exception is the superconducting transition temperature  $T_c$ , which is controlled by a logarithmic divergence with an upper cutoff set by the phonon frequency, and involves an interaction (the Coulomb pseudopotential) which has a logarithmic suppression with a lower cutoff set by the phonon frequency. The resulting, rather complicated, dependence of  $T_c$  on ion mass was determined by McMillan<sup>2</sup>.

A series of recent experimental papers reporting isotope effects (i.e. ion-mass dependence) for a variety of electronic properties<sup>3,4</sup> motivates re-examination of this issue. Of particular interest here are reports of a pronounced increase of the charge ordering transition temperatures of various members of the ‘CMR manganite’ family of manganese perovskites when <sup>18</sup>O is substituted for <sup>16</sup>O.<sup>5,6</sup> This leads us to re-examine the theory of charge density wave (CDW) instabilities in order to determine how the transition temperature  $T_{co}$  is affected by ion mass. A theory applicable to materials of current interest must go beyond the Migdal-Eliashberg approximation, must apply to the case of  $d = 3$  spatial dimensions and must be able to treat the physically relevant limit  $\gamma \ll 1$ .

The  $\Omega$ -dependence of  $T_{co}$  has been studied. In one

spatial dimension pioneering numerical work of Hirsch and Fradkin<sup>10</sup> followed by analytical studies by Bourbonnais and Caron<sup>11</sup> found a strong suppression of the zero temperature CDW order parameter with increasing  $\Omega$ . In  $d = 2$ <sup>12,13</sup> and  $d = \infty$ <sup>14</sup> the quantum phonon problem has been attacked by a direct numerical approach using quantum Monte Carlo (QMC) methods. However, numerical issues related to the mismatch between phonon and electron frequency scales however restricted the QMC studies<sup>12–14</sup> to the antiadiabatic limit,  $\Omega \sim t$ . Also, in Refs. 12–14 the isotope effect on the CDW transition temperature was not studied in detail, although values for  $T_{co}$  for a given phonon frequency were calculated. In  $d = \infty$  and for weak coupling strengths the CDW transition temperature is strongly reduced with decreasing ion mass and a reduction ratio of  $T_{co}(\Omega = 0.5t)/T_{co}(\Omega = 0) \approx 0.25$  has been reported.<sup>14,15</sup>

Especially in  $d = \infty$  considerable effort has been expended to construct weak-coupling perturbation theories which continuously connect the adiabatic to the antiadiabatic limit.<sup>14–17</sup> One important outcome of this work was the suggestion that future research should focus on generalizations of the ME theory that work with dressed phonons (renormalized ME) but include higher order non-adiabatic effects such as vertex corrections. Our method is such an approach. A large number of studies based on the Lang-Firsov<sup>18</sup> method have been published (see e.g. Ref. 19). For one dimensional systems the Lang-Firsov results are in agreement with previous work.<sup>20</sup> However, this is an uncontrolled approximation optimized for the single polaron problem and its applicability to metallic densities is not established.

In this paper we construct an essentially analytic theory of the charge density wave transition temperature in the physically relevant limit  $\gamma \ll 1$ . We build on previous work which showed how to construct an expansion in  $\gamma$  within the dynamical mean-field approximation<sup>8</sup> and

which analysed the classical limit ( $\Omega = 0$ ) of the charge density wave problem.<sup>9</sup> Here we show how to calculate  $T_{\text{co}}$  including the first non-Migdal term in  $\gamma$  for arbitrary values of  $\Omega/T_{\text{co}}$ . We find that  $T_{\text{co}}$  depends very strongly on  $\Omega$ , becoming very small as  $\Omega$  is increased (at fixed coupling) beyond the  $\Omega = 0$  value of  $T_{\text{co}}$ , but that the specific behavior depends strongly on whether spin-1/2 or spinless electrons are considered. For spinless electrons, relevant to half-metals such as CMR manganites, a divergent isotope exponent is obtained in the weak electron-phonon coupling limit.

## II. MODEL AND FORMALISM

In this paper we study the simplest model of electrons interacting with phonons, namely the Holstein model<sup>21</sup>  $H_{\text{Hol}} = H_{\text{el}} + H_{\text{ph}} + H_{\text{el-ph}}$  with

$$H_{\text{el}} = - \sum_{ij} t_{i-j} c_{i\sigma}^\dagger c_{j\sigma} - \mu \sum_i (c_{i\sigma}^\dagger c_{i\sigma} - n) , \quad (1)$$

$$H_{\text{ph}} = \frac{1}{2\Lambda} \sum_i (r_i^2 + \dot{r}_i^2/\Omega^2) , \quad (2)$$

$$H_{\text{el-ph}} = \sum_i r_i (c_{i\sigma}^\dagger c_{i\sigma} - n) \quad (3)$$

where we have absorbed the electron-phonon coupling into the phonon coordinate  $r$  which thus has dimension of energy as does the phonon stiffness parameter  $\Lambda$ . We further specialize to a mean electron density per spin direction of  $n = 1/2$ ; this implies  $\mu = 0$ . We also assume a bipartite lattice, which for our purposes we define as a lattice possessing a dispersion  $\epsilon_{\vec{k}}$  (Fourier transform of  $t_{i-j}$ ) and a wavevector  $\vec{Q}$  such that  $\epsilon_{\vec{k}-\vec{Q}} = -\epsilon_{\vec{k}}$  for all  $\vec{k}$  in the Brillouin zone. An equivalent definition is that the lattice may be divided into two sublattices  $A$  and  $B$ , such that  $t_{i-j}$  connects  $A$  sites only to  $B$  sites. The important feature of the dispersion is the bare density of states per site per spin  $\rho(\epsilon) = \frac{1}{N} \sum_{\vec{k}} \delta(\epsilon - \epsilon_{\vec{k}})$ . In this paper we use the semicircular form  $\rho(\epsilon) = \frac{1}{2\pi t^2} \sqrt{4t^2 - \epsilon^2}$ . It is useful to introduce the dimensionless electron-phonon coupling  $\lambda$  and adiabatic parameter  $\gamma$  by

$$\lambda = \Lambda \rho_0, \quad \gamma = \Omega \rho_0 . \quad (4)$$

Here  $\rho_0 = 1/\pi t$  denotes the bare density of states at the chemical potential.

We now establish notation by reviewing the derivation of the  $T_{\text{co}}$  equation within dynamical mean-field theory (DMFT). The fundamental assumption of DMFT is the momentum independence of the electron self energy  $\Sigma_n = \Sigma(i\omega_n)$  ( $\omega_n = 2\pi T(n+1/2)$ ). Consequently, in the absence of spatial symmetry breaking,  $\Sigma_n$  can be derived from an effective impurity model specified by the action

$$S(\{r_{nm}\}; \{c_n\}) = (T/2\Lambda) \sum_n r_{n0} (\omega_{n0}^2/\Omega^2 + 1) r_{0n}$$

$$-n \sum_n r_{n0} - (2s+1) \text{Tr} \ln [c_n \delta_{nm} - T r_{nm}] . \quad (5)$$

In this action  $r_{nm}$  are bosonic fields describing the phonons and  $c_n$  mean field functions describing the fermions (which have been integrated out). We have indexed the bosonic fields by the difference of two fermionic Matsubara frequencies  $\omega_{nm} = \omega_n - \omega_m$ . The factor  $(2s+1)$  takes the values one and two for spinless ( $s=0$ ) and spin-1/2 ( $s=1/2$ ) electrons, respectively. The partition function is the functional integral over the bosonic fields

$$Z = \int \mathcal{D}[r] \exp(-S) \quad (6)$$

and is a functional of the effective field  $c$  alone. It is useful to define the impurity Green's function  $\mathcal{G}$  and self energy  $\Sigma$  by

$$\mathcal{G}_n \equiv \frac{1}{2s+1} \frac{\delta \ln Z}{\delta c_n} \equiv \frac{1}{2s+1} \frac{1}{c_n - \Sigma_n(\{c_n\})} . \quad (7)$$

The effective field is fixed by equating the local Green's functions of the original lattice model and the effective impurity model. For a semicircular density of states one obtains

$$c_n = i\omega_n + \mu - t^2 \mathcal{G}_n(\{c_n\}) . \quad (8)$$

For temperatures below the CDW transition the self energy acquires two components for the two sublattices  $A$  and  $B$  which calls for two effective impurity models given by the effective fields  $a$  and  $b$  respectively. The resulting self-consistency equations are:

$$a_n = i\omega_n + \mu - t^2 \mathcal{G}_n(\{b_n\}) \quad (9)$$

$$b_n = i\omega_n + \mu - t^2 \mathcal{G}_n(\{a_n\}) . \quad (10)$$

Near the transition (assumed to be second order) we can expand  $a_n = c_n + \epsilon'_n$  and  $b_n = c_n - \epsilon'_n$  leading to  $\epsilon'_n = t^2 \sum_m \frac{\partial \mathcal{G}_n}{\partial c_m} \epsilon'_m$ . Making use of Eq. (7) we obtain

$$\epsilon'_n = \frac{1}{1 + (c_n - \Sigma_n)^2/t^2} \sum_m \frac{\partial \Sigma_n}{\partial c_m} \epsilon'_m . \quad (11)$$

It is convenient to rewrite Eq. (11) in the more symmetric form<sup>9,16</sup>

$$\epsilon_n = - \sum_m \chi_n^{1/2} \Gamma_{nm} \chi_m^{1/2} \epsilon_m . \quad (12)$$

Here we have introduced  $\chi_n = -\mathcal{G}_n/(i\omega_n - \Sigma_n)$ , the irreducible two particle vertex  $\Gamma_{nm} = \sum_{\sigma'} \partial \Sigma_n^\sigma / \partial \mathcal{G}_m^{\sigma'}$  and  $\epsilon_n = \epsilon'_n \chi_n^{1/2}$ . Eq. (12) is the statement that the matrix  $-\chi_n^{1/2} \Gamma_{nm} \chi_m^{1/2}$  has eigenvalue one and  $T_{\text{co}}$  is the temperature at which this eigenvalue problem has a solution. It can be easily shown<sup>16</sup> that  $\chi_n$  is the 'bare' CDW susceptibility of the original lattice model  $\chi_n = -1/N \sum_{\vec{k}} G_n(\vec{k} + \vec{Q}) G_n(\vec{k})$ .

### III. SOLUTION IN THE ADIABATIC LIMIT

As written, Eq. (12) is general, but not very useful because not only must the matrix be diagonalized numerically, but also determination of the matrix elements for arbitrary  $\lambda$  and  $\gamma$  requires performing the functional integral over phonon fields numerically (i.e. via quantum Monte Carlo) and this becomes prohibitively lengthy for physically relevant regimes of  $\Omega$  and  $T$ . Here we turn this difficulty to advantage, exploiting the smallness of  $\Omega$  and  $T$  to construct an analytic expansion in powers of  $\gamma$ . The expansion builds on the observation<sup>8</sup> that the biggest contribution to a diagram (e.g. for the electronic self energy or the vertex) with  $n$  phonon loops is of order  $[\max(T, \Omega)/t]^n$ . This can be seen as follows. A generic diagram  $D^{(n)}$  with  $n$  phonon loops contains  $n$  internal sums over bosonic Matsubara frequencies  $\omega_1, \dots, \omega_n$  (here  $\omega_n = \omega_{n0}$ ) each associated with one (or more) free phonon propagators given by

$$\mathcal{D}_n^0 = -\Lambda \frac{\Omega^2}{\Omega^2 + \omega_n^2}. \quad (13)$$

If  $F(i\omega_1, \dots, i\omega_n)$  depicts the appropriate product of Green's functions and phonon propagators we can write  $D^{(n)} = T^n \sum_{1, \dots, n} F(i\omega_1, \dots, i\omega_n)$ . In the classical limit,  $\Omega/T \rightarrow 0$ , the free phonon propagators become delta functions and therefore  $D^{(n)} \sim T^n$  as noted in Ref. 9. In the quantum case it is more appropriate to rescale the temperature  $\tilde{T} = T/\gamma$  leading to  $D^{(n)} = \gamma^n \tilde{T}^n \sum_{1, \dots, n} F(i\gamma\tilde{\omega}_1, \dots, i\gamma\tilde{\omega}_n)$ . The rescaled bosonic Matsubara frequencies  $\tilde{\omega}$  become continuous variables in the extreme quantum limit  $\tilde{T} \rightarrow 0$  and because  $F$  has a small frequency expansion we conclude that the biggest contributions to the  $n$  phonon loop diagram are of order  $\gamma^n$  as argued in Ref. 8. The diagrammatic expansion shown in Fig. 1 includes all terms with the minimal number of internal phonon loops, i.e. includes the leading nontrivial order for the electronic self energy and the vertex. Note that the leading order in  $\gamma$  contains both, the direct (first term in Fig. 1 (b)) and the exchange diagrams for the vertex. The conventionally defined ME approach<sup>12,14</sup> only sums the bubble diagrams for the CDW susceptibility, i.e. the exchange diagrams for the vertex (which we find to be of the same order) are neglected. Freericks and co-workers<sup>16,17,27</sup> have considered a variety of different vertex corrections to the conventionally defined ME approximation but they organized these in a coupling constant expansion and not in the small frequency expansion we considered here. Specific vertex corrections<sup>16</sup> are of higher order in  $\gamma$  than the ones treated in this work.

Adding the electron bubbles in Fig. 1 leads to a ‘dressed’ phonon propagator  $\mathcal{D}_n = [(\mathcal{D}_n^0)^{-1} - \Pi_n]^{-1}$  with a phonon self energy  $\Pi_n$  given by

$$\Pi_n = (2s+1)T \sum_m \mathcal{G}_{n+m} \mathcal{G}_m. \quad (14)$$

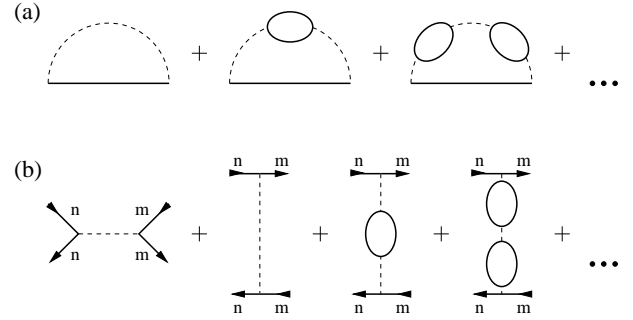


FIG. 1. Diagrammatic expansion of the one-particle self-energy (a) and of the irreducible vertex of the charge-order susceptibility (b) including all terms of order  $\bar{\gamma}$ . Heavy lines: full local Green's function  $\mathcal{G}_n$ . Dashed lines: free phonon propagator. All other possible diagrams are smaller by additional factors of  $\bar{\gamma}$  and are not shown.

The occurrence of the free phonon propagator restricts the bosonic Matsubara frequencies  $\omega_n$  to values on the scale of  $\Omega$ . Following the arguments given in Ref. 8 we assume that the *dominant* contributions to  $\Pi_n$  come from frequencies of order  $t$  and consequently set the index  $n$  under the sum to zero.<sup>8</sup> To leading order in  $\gamma$  we can replace the full by the free Green's function and find  $\Pi_n = -1/\Lambda_c + \mathcal{O}(T^2)$  with  $\Lambda_c = 3/[4(2s+1)\rho_0]$ .<sup>8,9</sup> The ‘dressed’ phonon propagator reads

$$\mathcal{D}_n = -\bar{\Lambda} \frac{\bar{\Omega}^2}{\bar{\Omega}^2 + \omega_n^2} \quad (15)$$

with the renormalized phonon stiffness and phonon frequency

$$\bar{\Lambda} = \Lambda/(1 - \Lambda/\Lambda_c) \quad (16)$$

$$\bar{\Omega} = \Omega(1 - \Lambda/\Lambda_c)^{1/2}. \quad (17)$$

Due to this influence of the electrons on the phonons the given expansion is actually an expansion in  $\bar{\lambda} = \bar{\Lambda}\rho_0$  and  $\bar{\gamma} = \bar{\Omega}\rho_0$ . Maybe a more familiar way to express the dressed electron phonon coupling is  $\bar{\lambda} = \rho_0 \Lambda \mathcal{D}(0)$ . The importance of not neglecting the renormalization of phonons by electrons was stressed by several authors, both in studies of  $d = 2^{12,13}$  and  $d = \infty^{14,22}$  spatial dimensions. In the limit  $\Lambda \rightarrow \Lambda_c$  the renormalized phonon stiffness  $\bar{\Lambda} \rightarrow \infty$  and the renormalized phonon frequency  $\bar{\Omega} \rightarrow 0$  signaling that the lattice becomes unstable against *local* distortions. In the absence of long range order the ground state expectation value of the lattice distortion  $\langle r \rangle$  would change from  $\langle r \rangle = 0$  for  $\Lambda < \Lambda_c$  to  $\langle r \rangle \neq 0$  for  $\Lambda > \Lambda_c$ . This polaronic instability has been extensively discussed in Ref. 22 and it is important to note that the coupling constant is strongly enhanced and the adiabatic parameter is strongly suppressed near the instability.

Within the small  $\gamma$  limit we obtain

$$\Gamma_{nm} = \frac{T}{\rho_0} \left[ -(2s+1)\lambda + \bar{\lambda} \frac{1}{1 + \bar{\omega}_{nm}^2} \right] + \mathcal{O}(\max[T^2/t^2, \bar{\gamma}^2]) \quad (18)$$

and

$$\Sigma_n = \frac{\bar{\lambda}T}{\rho_0} \sum_m \mathcal{G}_m \frac{1}{1 + \tilde{\omega}_{nm}^2} + \mathcal{O}(\max[T^2/t^2, \bar{\gamma}^2]). \quad (19)$$

Here, we have rescaled the bosonic frequencies  $\tilde{\omega}_{nm} = \omega_{nm}/\bar{\Omega}$ . In Eq. (19) as well as in  $\chi_n$ , we can replace the full Green's function by the bare one  $\mathcal{G}_n \rightarrow \mathcal{G}_n^0 = [i\omega_n - i\text{sgn}(\omega_n)\sqrt{\omega_n^2 + 4t^2}]/2t^2$  to leading order in  $\bar{\gamma}$ . Previous studies<sup>23</sup> asserted that for small phonon frequencies vertex corrections such as the second term in Eq. (18) can be neglected. We see that this is not quite correct: rather, the vertex corrections for  $\bar{\gamma} \rightarrow 0$  affect only the diagonal elements of the matrix in Eq. (12), but in this diagonal region they are of the same order as the contribution from the first part of Eq. (18).

The importance of the vertex corrections has been demonstrated in the classical limit<sup>9</sup>. For  $\bar{\gamma} \rightarrow 0$  ( $\bar{\Omega} \rightarrow 0$ ) we can expand

$$\frac{1}{1 + \tilde{\omega}_{nm}^2} \approx \delta_{nm} + \frac{1}{\tilde{\omega}_{nm}^2} (1 - \delta_{nm}) \rightarrow \delta_{nm}, \quad (20)$$

i.e. the phonon propagator becomes diagonal for  $\bar{\gamma} = 0$ . In this limit both vertex and self energy corrections to the BCS case modify the upper cutoff of the logarithmic divergence in the CDW susceptibility leading to a suppression of the CDW transition temperature, which has been interpreted in terms of inelastic scattering of electrons by phonons.<sup>9</sup>

Returning now to the quantum problem we insert Eq. (18) into the eigenvalue equation (12) yielding

$$\epsilon_n = \chi_n^{1/2} (2s+1) \frac{\lambda T}{\rho_0} \sum_m \chi_m^{1/2} \epsilon_m - \chi_n^{1/2} \frac{\bar{\lambda} T}{\rho_0} \sum_m \frac{1}{1 + \tilde{\omega}_{nm}^2} \chi_m^{1/2} \epsilon_m. \quad (21)$$

For generic values of  $\Omega/T_{\text{co}}(0)$  we solve Eq. (21) numerically by restricting the sums to a finite range  $m < N$  and diagonalizing the resulting matrix exactly numerically. Convergence is improved by using an analytical approximation for Eq. (21) for large frequencies  $\omega_n > \omega_N$ . In the large frequency limit the sums in Eq. (19) and Eq. (21) including the phonon propagator equal their  $n = m$  values times the factor  $T \sum_m 1/(1 + \tilde{\omega}_m^2) = (\bar{\Omega}/2) \coth(\bar{\Omega}/2T)$ . Therefore, the coupling constant  $(2s+1)\lambda$  can be replaced by the effective coupling constant

$$\lambda^* = (2s+1)\lambda/[1 - (2s+1)\lambda I] \quad (22)$$

with

$$I = \frac{T}{\rho_0} \sum_{|n|>N} \frac{1}{(\chi_n^0)^{-1} + (\bar{\lambda}\bar{\Omega}/\rho_0) \coth(\frac{\bar{\Omega}}{2T})} \quad (23)$$

where we have introduced  $\chi_n^0 = -\mathcal{G}_n^0/i\omega_n$ . For  $n, m = 0, \dots, N$  the leading eigenvalue of the matrix

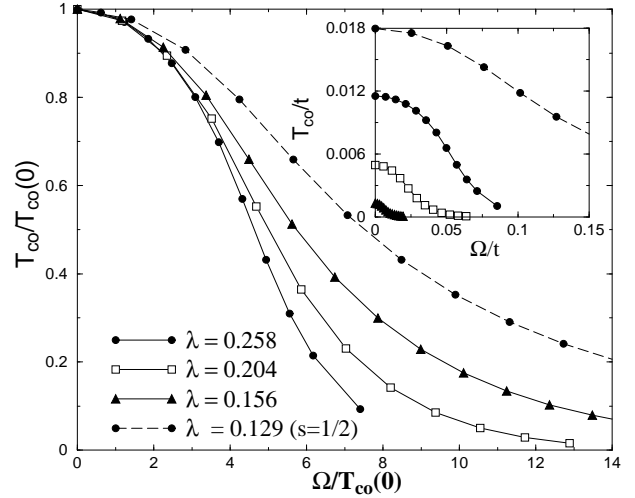


FIG. 2. CDW transition temperature as function of the typical phonon frequency  $\Omega \sim M^{-1/2}$  for spinless electrons. In the main panel  $T_{\text{co}}$  and  $\Omega$  are scaled to the zero frequency value of the CDW transition temperature  $T_{\text{co}}(0)$ . Circles connected with dashed lines represent results for  $\lambda = 0.129$  but spin  $s = 1/2$ . Inset:  $T_{\text{co}}$  as function of  $\Omega$  on the scale  $t$ .

$$M_{nm} = \frac{2\lambda^* T}{\rho_0} \chi_n^{1/2} \chi_m^{1/2} - \frac{\bar{\lambda} T}{\rho_0} \chi_n^{1/2} \chi_m^{1/2} \times \left\{ \frac{1}{1 + [2\pi(n-m)T/\bar{\Omega}]^2} + \frac{1}{1 + [2\pi(n+m)T/\bar{\Omega}]^2} \right\} \quad (24)$$

has to be found.  $T_{\text{co}}$  is given by the condition that the leading eigenvalue equals one. We have checked the convergence with  $N$ ; typically we used values ranging from  $N = 256$  to  $N = 4096$  yielding a relative error  $\delta T_{\text{co}}/T_{\text{co}} < 0.01$ . For later use we give the weak coupling  $\bar{\lambda} \rightarrow 0$  result for the effective coupling constant. In this limit the charge density wave transition temperature becomes very small and the Matsubara sum can be evaluated as an integral yielding  $1/\lambda^* \approx 1/[(2s+1)\lambda] - \ln(2t/\omega_N)$ .

#### IV. RESULTS

The CDW transition temperature resulting from a numerical diagonalization of (24) is shown in Fig. 2. Decreasing the ionic mass, i.e. increasing the phonon frequency  $\Omega$ , is seen to suppress  $T_{\text{co}}$  considerably for both spinless and spin-1/2 electrons. The suppression becomes very pronounced when  $\Omega \sim (2s+1)\pi T_{\text{co}}(\Omega=0)$ . This is in qualitative agreement with the strong suppression of the zero temperature order parameter reported in  $d = 1$  where the CDW state is destroyed when the phonon frequency is of the order of the adiabatic ( $\gamma = 0$ ) mean-field gap value.<sup>24</sup> We note that the scaled  $T_{\text{co}}$  curves fan out at larger phonon frequencies: in the extreme quantum limit the suppression of  $T_{\text{co}}(\Omega)$  relative to  $T_{\text{co}}(\Omega=0)$  depends strongly on coupling. This is an indication that quantum non-Migdal effects (high energy electron self energy

$\Sigma_n \approx 1/2 \bar{\Lambda} \bar{\Omega} \mathcal{G}_n^0$ ) are different from classical non-Migdal effects ( $\Sigma_n \approx \bar{\Lambda} T \mathcal{G}_n^0$ ).

$T_{\text{co}}(0)$  increases considerably for spin  $s = 1/2$ , essentially because the spin sum increases the bare susceptibility by a factor of two. Nevertheless, the change in spin  $s$  cannot be accounted for by a change of  $\lambda$  (i.e.  $\rho_0$ ) only. Reducing  $\lambda$  by a factor of two when changing the spin from  $s = 0$  to  $s = 1/2$  does not bring the transition temperature curves close to each other as shown in the inset of Fig. 2 (see the circles connected with a solid,  $s = 0$ , or dashed,  $s = 1/2$ , line). The rather different suppression of  $T_{\text{co}}$  for  $s = 0$  and  $s = 1/2$  was also found in studies in  $d = 1$ .<sup>10,11</sup> Even on the scale  $T_{\text{co}}(0)$  the large frequency tails are qualitatively different in the two cases. We provide some analytic insight in Section V.

Within the spin-1/2 Holstein model sizable transition temperatures might be obtained even in the antiadiabatic limit and for modest coupling strengths making the CDW transition accessible to QMC simulations. Freericks and Jarell report a suppression of  $T_{\text{co}}/T_{\text{co}}(0) \approx 0.25$  for  $\Omega/T_{\text{co}}(0) \approx 7.1$  (corresponding to  $\gamma = 0.282$ ).<sup>14</sup> This result, obtained numerically in the antiadiabatic limit, indicates an even stronger suppression of  $T_{\text{co}}$  than obtained here in the adiabatic limit ( $\gamma$  values used in our calculation vary from 0 to 0.08) but is of the same order. The comparison of absolute numbers is difficult because the work Ref. 14 does not use the semicircular density of states we have chosen.

It is important to note that  $T_{\text{co}}(0)$  is not the mean-field CDW transition temperature  $T_{\text{co}}^{\text{MF}} = (8t\gamma/e\pi) \exp[-1/(2s+1)\lambda]$ .<sup>9</sup> Even at zero phonon frequency the charge density wave transition temperature is suppressed by thermal fluctuations of the phonon fields, e.g.  $T_{\text{co}}(0)/T_{\text{co}}^{\text{MF}} = 0.33, 0.40, 0.49$  for  $s = 0$  and  $\lambda = 0.258, 0.204, 0.156$  respectively. In Fig. 3  $T_{\text{co}}$  is plotted as function of the coupling constant  $\lambda$ . The suppression of the charge density wave transition temperature relative to its ‘BCS’ or static mean field value due to thermal fluctuations (white circle) and due to additional quantum fluctuations (white squares) is clearly visible. At weak coupling quantum fluctuations of the phonon fields are so effective in reducing  $T_{\text{co}}$  that it seems unlikely that CDW materials can be found with a Debye temperature  $\Theta_{\text{D}}$  much larger than the mean field transition temperature  $T_{\text{co}}^{\text{MF}}$ . Higher order corrections in  $\bar{\gamma}$  are accompanied by higher powers of  $\bar{\lambda}$  and can no longer be neglected when the coupling constant is large. The comparison with the full numerical solution of the classical DMFT equation given in Ref. 9 reveals that the expansion suggested here breaks down already at the surprisingly small value of  $\bar{\gamma}\bar{\lambda} \approx 10^{-2}$ . The inset of Fig. 3 will be discussed in Section VI.

The dependence of the CDW transition temperature on the ionic mass is usually discussed in terms of the isotope exponent  $\alpha = \frac{1}{2} \frac{\Omega}{T_{\text{co}}} \frac{dT_{\text{co}}}{d\Omega}$  which is shown in Fig. 4. Because of the rapidly increasing factor  $\Omega/T_{\text{co}}$  the negative isotope exponent  $-\alpha$  monotonically increases to very

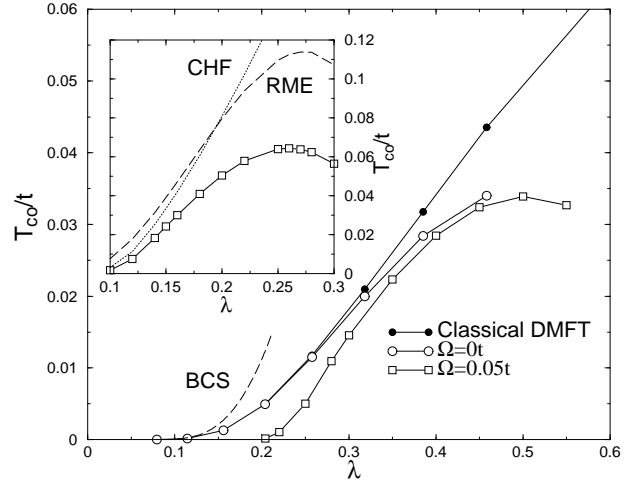


FIG. 3. Charge density wave transition temperature as function of the coupling strength  $\lambda$  for  $s = 0$ , calculated from Eq. (21) for  $\gamma = 0$  (white circles, identical to the modified BCS approximation of Ref. 9) and  $\gamma = 0.05/\pi$  (white squares). Also shown are the ‘BCS’ approximation<sup>9</sup> (dashed line) and a numerical solution of the classical DMFT equations.<sup>9</sup> For  $\lambda = 0.35$  ( $\bar{\lambda}\bar{\gamma} = 7.6 \times 10^{-3}$ ) differences (amplified because  $T_{\text{co}}$  depends exponentially on parameters) between the exact classical treatment and our approximate results become noticeable, suggesting that the expansion breaks down. The inset presents data for  $s = 1/2$  and  $\gamma = 0.1/\pi$ . The solution of Eq. (21) (white squares) is compared to the renormalized Migdal-Eliashberg theory (RME) and to the conserving Hartree-Fock approximation (CHF) discussed in Ref. 14. The  $\bar{\gamma}$  expansion can be trusted up to  $\lambda = 0.18$  which corresponds to  $\bar{\lambda}\bar{\gamma} = 7.9 \times 10^{-3}$ . For details see text.

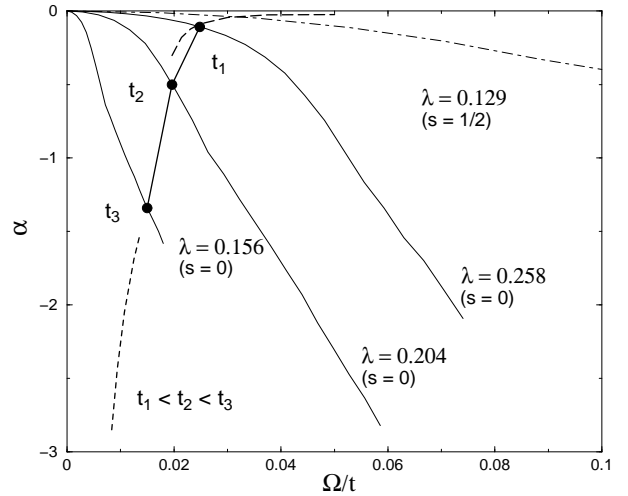


FIG. 4. Isotope exponent as function of  $\Omega/t$  for spinless electrons. With increasing phonon frequency  $\alpha$  drops to huge negative values. The circles connected with a thick solid line represents the change in  $\alpha$  with increasing  $t$  for fixed values of  $\Lambda = 0.49$  and  $\Omega = 0.015$ . ( $t_1 = 1.65, t_2 = 1.31, t_3 = 1$ ) The dashed and dotted line are extrapolations given by Eq. (28) and Eq. (32), respectively. In the latter we have used a cutoff parameter  $\eta = 1.16$ . The isotope exponent for spin-1/2 electrons (dot-dashed line) remains finite.

large values for spinless electrons. In the case  $s = 1/2$ , however, the isotope exponent flattens off as function of  $\Omega/t$  due to the different large frequency behavior of  $T_{\text{co}}$ .

## V. ANALYTIC EXPRESSIONS

In the adiabatic and extreme quantum limits we can derive explicit analytic expressions for  $T_{\text{co}}$ . First, we consider the limit  $\Omega/T_{\text{co}}(\Omega = 0) \rightarrow 0$ , i.e. we expand (21) around the classical solution obtained in Ref. 9. An appropriate Ansatz for the eigenvector  $\epsilon_n$  is

$$\epsilon_n = \mathcal{C} \frac{\chi_n^{1/2}}{[1 + (\bar{\lambda} T/\rho_0) \chi_n]} . \quad (25)$$

Note that,  $\epsilon_n$  is not quite the classical solution because it still depends on  $\bar{\gamma}$  via  $\chi_n$ . Therefore, after inserting (25) into (21) we still have to expand in  $\bar{\gamma}$  which finally leads to

$$\frac{1}{2s+1} = \frac{\lambda T}{\rho_0} \sum_n \frac{\chi_n^{\text{class}}}{1 + (\bar{\lambda} T/\rho_0) \chi_n^{\text{class}}} - \lambda K \left( \frac{\Omega}{T_{\text{co}}(0)} \right)^2 \quad (26)$$

with  $\chi_n^0 = (\sqrt{(2t/\omega_n)^2 + 1} - 1)/2t^2$ .  $K$  is a numerical coefficient independent of temperature but weakly dependent on  $\bar{\lambda}$ . Its magnitude is relatively small, e.g.  $K = 1.775 \times 10^{-2}$  for  $\lambda = 0.156$  ( $s = 0$ ).

The first part of Eq. (26) is the classical  $T_{\text{co}}$  equation.<sup>9</sup> The sum has a logarithmic  $T$  dependence. Therefore, expanding  $T = T_{\text{co}}(0) - \delta T$  leads to a term  $[\lambda/T_{\text{co}}(0)] \delta T$ . Consequently, the CDW transition temperature in the limit  $\Omega/T_{\text{co}}(0) \ll 1$  is given by

$$\frac{T_{\text{co}}}{T_{\text{co}}(0)} = 1 - K \left( \frac{\Omega}{T_{\text{co}}(0)} \right)^2 . \quad (27)$$

The quadratic drop is clearly seen in Fig. 2. We can use Eq. (27) to derive the isotope exponent in the classical limit. We obtain

$$\alpha = -K \left( \frac{\Omega}{T_{\text{co}}(0)} \right)^2 = \frac{T_{\text{co}}}{T_{\text{co}}(0)} - 1 . \quad (28)$$

The isotope exponent as function of  $t$  according to this result is depicted in Fig. 4 as a dashed line. The exponential decrease of  $T_{\text{co}}(0)$  with increasing kinetic energy  $t$  of the electrons is responsible for the sharp upturn of the negative isotope exponent.

In the extreme quantum limit the temperature is not a relevant high energy scale. Therefore, the upper cutoff frequency introduced above should be given by  $\omega_N = \eta \bar{\Omega}$  to yield results to logarithmic precision with  $\eta$  being a numerical factor of order one. We can replace the phonon propagator by

$$\frac{1}{1 + \tilde{\omega}_{nm}^2} \approx 1 - \tilde{\omega}_{nm}^2 . \quad (29)$$

Moreover, to the same precision all Matsubara sums can be replaced by integrals and the temperature occurs only as a lower cutoff in the theory. The  $T_{\text{co}}$  equation (21) reads simply

$$1 = (\lambda^* - \bar{\lambda}) t \int_T^{\eta \bar{\Omega}} \chi(\omega) d\omega . \quad (30)$$

For small frequencies the self energy (19) is given by  $\Sigma_n = -i\omega_n \bar{\lambda}$ . Therefore,  $\chi(\omega) = \chi_0(\omega)/(1 + \bar{\lambda})$  which, inserted in Eq. (30), gives the CDW transition temperature in the limit  $\Omega/T_{\text{co}} \gg 1$

$$T_{\text{co}} = \eta \bar{\Omega} \exp \left( -\frac{1 + \bar{\lambda}}{\lambda^* - \bar{\lambda}} \right) \equiv \eta \bar{\Omega} \exp \left( -\frac{1}{\lambda_{\text{eff}}} \right) . \quad (31)$$

Note that,  $\bar{\Omega}$  enters the calculation as the upper cutoff of the integral (30) and as lower cutoff in the effective interaction strength  $\lambda^*$  (see (22)) in close resemblance to the well known McMillan formula for the superconducting transition temperature.<sup>2</sup> Because the effective coupling constant  $\lambda_{\text{eff}}$  depends logarithmically on  $\bar{\Omega}$  (via  $\lambda^*$ ) we obtain for the isotope exponent in the extreme quantum limit

$$\alpha = \frac{1}{2} \left[ 1 - \frac{1 + \bar{\lambda}}{(1 - \bar{\lambda}/\lambda^*)^2} \right] . \quad (32)$$

The extreme quantum limit for fixed values of the phonon frequency  $\Omega$  is realized for small values of  $\lambda$  (or large values of  $t$ ) due to the fast drop of  $T_{\text{co}}(0)$  with decreasing coupling strength (see Fig. 3). For spinless electrons the isotope exponent becomes  $\alpha \approx -1/(2\lambda^2 I^2)$ , i.e.  $\alpha$  diverges in the limit  $\lambda \rightarrow 0$  with power law behavior. The divergence of the negative isotope exponent with increasing kinetic energy of the electrons is shown in Fig. 4 as a dotted line. The isotope exponent for spin-1/2 electrons, however, remains finite, equalling  $\alpha = -3/2$  for  $\lambda \rightarrow 0$ . The difference between the cases  $s = 0$  and  $s = 1/2$  is due to a near-cancellation of the vertex parts for  $s = 0$ . Consequently, the leading order of  $\lambda_{\text{eff}}$  is  $\mathcal{O}(\lambda^2)$  for  $s = 0$  and  $\mathcal{O}(\lambda)$  for  $s = 1/2$ .

In the ME theory for the superconducting transition temperature the effect of Coulomb interaction is considered by introducing a pseudopotential  $\mu^*$ .<sup>2</sup> Therefore, it is tempting to absorb Coulomb effects on the charge density wave transition temperature in a similar way in  $\lambda^*$ . Indeed, a repulsive Coulomb interaction is an electron-electron interaction similar to the attractive vertex part, first term in Fig. 1(b), and will change the value of  $\lambda^*$  simply by replacing  $(2s+1)\lambda \rightarrow (2s+1)\lambda - U$  (see also Ref. 26).  $\lambda^*$  acts as a pseudopotential with a non vanishing value for  $U = 0$ . Nevertheless, Coulomb interaction will also change the electron self energy and the ‘vertex corrections’ (second and following terms in Fig. 1(b)) which is a more subtle effect due to the different frequency dependence of electron-phonon and Coulomb interactions and is left for future work.

## VI. RELATION TO TRADITIONAL APPROACHES

It is traditional to write the CDW transition temperature in the form  $T_{\text{co}} = W_{\text{eff}} \exp(-1/\lambda_{\text{eff}})$  defining an effective bandwidth and coupling constant. The effective parameters  $W_{\text{eff}}$  and  $\lambda_{\text{eff}}$  are usually obtained by fitting to experimental data and therefore the functional dependence on the microscopic properties like electron-phonon coupling and adiabatic parameter remains hidden. The isotope exponent, however, explores this dependence and tests our physical understanding of the CDW transition.

A ‘BCS’ or static mean field approach<sup>25</sup> would result in  $T_{\text{co}}^{\text{MF}} = 2t \exp[-1/(2s+1)\lambda]$ , i.e.  $T_{\text{co}}$  depends exponentially on  $\lambda$  but is independent of  $\gamma$ . For strong coupling the ‘BCS’ theory is clearly wrong because the Holstein model in this limit can be mapped on an effective pseudospin model<sup>10</sup> and  $T_{\text{co}}$  has to decrease with increasing  $\lambda$ . Here we have demonstrated that also the weak coupling behavior is not predicted correctly and that instead of an ‘BCS’ isotope exponent  $\alpha = 0$  an enhanced ( $s = 1/2$ ) or even divergent ( $s = 0$ ) negative isotope effect is obtained.

Corrections to the BCS approximation have been considered. In the conventional Migdal-Eliashberg (ME) theory<sup>1</sup> of electron-phonon effects in solids electron self energies arising from the interaction with the phonons are included but all vertex corrections are neglected. Other authors<sup>12,14</sup> have argued that one should include also the feedback of the electrons on the phonon system but still neglecting the vertex corrections, thus defining a renormalized Migdal-Eliashberg theory (RME). In our notation this corresponds to dropping the second ( $\bar{\lambda}$ ) term in Eq. (21). The RME approximation predicts an incorrect isotope effect because  $T_{\text{co}}$  depends on ion mass only via the dependence of  $\chi_m$  on the normal state self energy, and comparison to our results shows that this dependence is not the leading one. At very weak coupling the RME theory reduces to the BCS theory (up to logarithmic corrections) and predicts  $\alpha = 0$ . Freericks and co-workers added extra vertex corrections to the RME theory<sup>16</sup> but these are higher order in  $\gamma$  than the effects we studied in this paper.

We have plotted the charge density wave transition temperature for various coupling strengths  $\lambda$  and fixed adiabatic parameter  $\gamma = 0.1/\pi$  and  $s = 1/2$  in the inset of Fig. 3 for both the RME approach and the present work. The charge density wave transition temperature obtained within RME theory is always larger than the one obtained from the systematic  $\bar{\gamma}$  expansion presented here. A similar plot for a larger value of  $\gamma = 0.5/\sqrt{\pi}$  has been presented in Ref. 14, where the RME results were compared with QMC data, showing that the RME theory indeed overestimates the transition temperature for weak coupling strength at least in the antiadiabatic limit. Note that, the RME results presented in Ref. 14 are not precisely identical to ours because we have included the phonon self energy only to leading order in  $\bar{\gamma}$ ,

but we believe that this does not effect the conclusions drawn here. It is well known that  $T_{\text{co}}(\lambda)$  is maximized at a  $\lambda_{\text{max}} < \infty$ . [ $T_{\text{co}} \rightarrow 0$  as  $\lambda \rightarrow 0$  because the coupling vanishes;  $T_{\text{co}} \rightarrow 0$  as  $\lambda \rightarrow \infty$  because in this limit a picture of almost completely localized particles with intersite interactions  $\sim t^2/\lambda$  applies.] The present approach underestimates both  $\lambda_{\text{max}}$  and  $T_{\text{max}}$ , as may be seen (Fig. 3) by comparison to the classical treatment of Ref. 9 (to which the present treatment reduces as  $T_{\text{co}}$  becomes greater than  $\Omega$ ) and by comparison to QMC data (Ref. 14) and indeed is not expected to apply for  $\lambda \sim \lambda_{\text{max}}$ .

A theory neglecting the renormalization of the phonon propagator by electrons predicts that  $T_{\text{co}}$  is maximized at  $\lambda = \infty$ . As an example we have plotted in the inset of Fig. 3 the conserving Hartree-Fock approximation discussed by Freericks *et al.*<sup>14</sup> This corresponds to using Eq. (21) but with  $\bar{\lambda}$  replaced by  $\lambda$ . In the weak coupling limit the difference between  $\bar{\lambda}$  and  $\lambda$  is negligible, so the CHF theory gives a good estimate of the CDW transition temperatures. The comparison with QMC data given in Ref. 14 demonstrate that the CHF theory, and therefore the theory given here, can (at least for  $s = 1/2$  and weak coupling strengths) be extended to the antiadiabatic limit.

Finally, we point out that the systematic expansion in  $\bar{\gamma}$  discussed in this work reproduces the results of the renormalized ME theory when applied to the calculation of the superconducting transition temperature  $T_c$ . Following Freericks and Scalapino<sup>27</sup> we find  $T_c \approx \eta \Omega \exp[-(1 + \bar{\lambda})/\bar{\lambda}]$  in the extreme quantum limit. For the half-filled Holstein model the charge density wave transition temperature is always larger than the superconducting transition temperature if  $\Omega < \infty$ ; only as  $\Omega \rightarrow \infty$  do they become equal.<sup>23</sup> The superconducting transition temperature is controlled by a logarithmic divergence with upper cutoff set by the phonon frequency whereas the corresponding upper cutoff in the theory for  $T_{\text{co}}$  is enhanced towards  $2t$  by the first diagram in Fig. 1(b).

## VII. CONCLUSION AND COMPARISON TO EXPERIMENT

We have used the dynamical mean field method to obtain a systematic and tractable treatment of the isotope effect on charge density wave transitions. Our method is applicable to the physically relevant case in which both phonon frequency and transition temperature are small relative to the electronic bandwidth, and in combination with the results of Ref. 8 may be generalized to the crucial case in which other interactions beyond the electron-phonon one are important.

Quantum phonon effects are found to suppress the charge density wave transition temperature severely. This is in agreement with previous work on one dimensional models demonstrating that the suppression of  $T_{\text{co}}$

is not due to the strong quantum fluctuations characteristic of one spatial dimension. The isotope exponent of  $T_{co}$  for spin-1/2 electrons is enhanced compared to the ME prediction. In the case of spinless electrons the isotope exponent may even be divergent. Although beyond the scope of the theory, the consideration of phonon self energy effects lead to an optimal charge density wave transition temperature for values of the coupling strength slightly below the polaronic instability at  $\lambda_c$  but peak position and height are underestimated.

Our results suggest that it will be difficult to find CDW systems with mean field transition temperatures much less than typical Debye frequencies. It is of interest to examine data with this in mind. For quasi-one-dimensional CDW materials the *mean field* CDW transition temperature is typically larger than room temperature and therefore larger than or of the same order as the Debye temperature  $\Theta_D$ . In TaS<sub>3</sub>, K<sub>0.3</sub>MoO<sub>3</sub> and (TaSe<sub>4</sub>)<sub>2</sub>I one deduces experimentally values of  $T_{co}^{MF} \approx 540K$ ,  $T_{co}^{MF} \approx 330$  and  $T_{co}^{MF} \approx 1040K$  respectively.<sup>25</sup> Quasi-two-dimensional CDW materials include the dichalcogenides and the molybdenum bronzes and oxides. For these materials it is more difficult to deduce mean field values of the CDW transition temperature because the CDW transition is not accompanied by a metal insulator transition. For  $2H - TaSe_2$  one might argue from measurements of the optical conductivity<sup>28</sup> for a value of  $T_{co}^{MF} \approx 580K$  similar to the quasi-one-dimensional materials. Charge order transitions are also observed in many two and three dimensional transition metal oxides including some members of the high-temperature superconductor and ‘CMR’ family.<sup>29</sup> Frequently, the Coulomb repulsion of the charge carriers is responsible for the charge order transition and therefore beyond the scope of this paper. Nevertheless, the phenomenology is very similar and e.g. for La<sub>1.67</sub>Sr<sub>0.33</sub>NiO<sub>4</sub> one might deduce  $T_{co}^{MF} = 750K$ . As was suggested by our theory the case of  $\Theta_D \gg T_{co}^{MF}$  seems to be extremely rare.

Our results bear at least a qualitative similarity to data obtained on ‘CMR’ manganites. Recently, a colossal isotope shift of the CDW transition temperature in Nd<sub>0.5</sub>Sr<sub>0.5</sub>MnO<sub>3</sub> was reported.<sup>6</sup> With magnetic field the negative isotope exponent varies from  $\sim 1.2$  to  $\sim 4.5$ . Within the double exchange picture of the manganites an increase of the applied magnetic field means an increase of the kinetic energy  $t$ . Due to the large Hund’s rule coupling of the conduction electron spins to the core spins of the Mn ions the conduction electrons are fully spin polarized. Therefore we should compare to the case  $s = 0$ . To demonstrate the effect of an increasing  $t$  in our calculation we draw a line for fixed  $\Lambda$  and  $\Omega$  in Fig. 4. Indeed, we find a monotonically increasing negative isotope effect with increasing  $t$ .

*Acknowledgements.* We thank A. Deppeler and M. Gros for useful discussions. SB acknowledges the DFG, the Rutgers University Center for Materials Theory and NSF DMR0081075 for financial support; AJM acknowl-

edges NSF DMR0081075.

- 
- <sup>1</sup> A.B. Migdal, Sov. Phys. JETP **7**, 996 (1958); G.M. Eliashberg, Sov. Phys. JETP **11**, 696 (1960)
  - <sup>2</sup> W.L. McMillan, Phys. Rev. **167**, 331 (1968)
  - <sup>3</sup> see e.g. G.M. Zhao, K. Conder, H. Keller and K.A. Müller, Nature **381**, 676 (1996); J.P. Franck *et al.*, Phys. Rev. B **58**, 5189 (1998); G.M. Zhao, K. Conder, H. Keller and K.A. Müller, Phys. Rev. B **60**, 11914 (1999); A.K. Heilmann *et al.*, Phys. Rev. B **61**, 8950 (2000); G.M. Zhao, K. Conder, H. Keller and K.A. Müller, Phys. Rev. B **62**, 5334 (2000)
  - <sup>4</sup> see e.g. N.A. Babushkina *et al.*, Nature **391**, 159 (1998); A.M. Balagurov *et al.*, Phys. Rev. B **60**, 383 (1999);
  - <sup>5</sup> I. Isaac and J.P. Franck, Phys. Rev. B **57**, R5602 (1998)
  - <sup>6</sup> G.M. Zhao, K. Ghosh and R.L. Greene, J. Phys.: Condens. Matter **10**, L737 (1998)
  - <sup>7</sup> A. Georges, G. Kotliar, W. Krauth and M. Rozenberg, Rev. Mod. Phys. **68**, 13 (1996)
  - <sup>8</sup> A. Deppeler and A.J. Millis, cond-mat/0004200
  - <sup>9</sup> S. Blawid and A.J. Millis, Phys. Rev. B **62**, 2424 (2000)
  - <sup>10</sup> J.E. Hirsch and E. Fradkin, Phys. Rev. B **27**, 4302 (1983)
  - <sup>11</sup> C. Bourbonnais and L.G. Caron, J. Phys. France **50**, 2751 (1989)
  - <sup>12</sup> F. Marsiglio, Phys. Rev. B **42**, 2461 (1990)
  - <sup>13</sup> R.M. Noack, D.J. Scalapino and R.T. Scalettar, Phys. Rev. Lett. **66**, 778 (1991); R.M. Noack and D.J. Scalapino, Phys. Rev. B **47**, 305 (1993)
  - <sup>14</sup> J.K. Freericks, M. Jarrell, D.J. Scalapino, Phys. Rev. B **48**, 6302 (1993)
  - <sup>15</sup> J.K. Freericks, V. Zlatić and M. Jarrell, Phys. Rev. B **61**, R838 (2000)
  - <sup>16</sup> J.K. Freericks, Phys. Rev. B **50**, 403 (1994); J.K. Freericks and M. Jarrell, Phys. Rev. B **50**, 6939 (1994)
  - <sup>17</sup> J.K. Freericks, V. Zlatić, W. Chung and M. Jarrell, Phys. Rev. B **58**, 11613 (1998)
  - <sup>18</sup> I.G. Lang and Yu.A. Firsov, Sov. Phys. JETP **16**, 1301 (1963)
  - <sup>19</sup> A.S. Alexandrov and N.F. Mott, *Polarons and Bipolarons* (World Scientific, Singapore, 1995)
  - <sup>20</sup> H. Zheng, D. Feinberg and M. Avignon, Phys. Rev. B **39**, 9405 (1989)
  - <sup>21</sup> T. Holstein, Ann. Phys. **8**, 325 (1959); Ann. Phys. **8**, 343 (1959)
  - <sup>22</sup> A.J. Millis, R. Mueller and B.I. Shraiman, Phys. Rev. B **54**, 5389 (1996)
  - <sup>23</sup> S. Ciuchi, F. de Pasquale, C. Masciovecchio and D. Feinberg, Europhys. Lett. **24**, 575 (1993); S. Ciuchi and F. de Pasquale, Phys. Rev. B **59**, 5431 (1999)
  - <sup>24</sup> R.J. Bursill, R.H. McKenzie and C.J. Hamer, Phys. Rev. Lett. **80**, 5607 (1998)
  - <sup>25</sup> G. Grüner, *Density Waves in Solids* (Addison-Wesley, New York, 1994)
  - <sup>26</sup> J.K. Freericks and M. Jarrell, Phys. Rev. Lett. **75**, 2570 (95)
  - <sup>27</sup> J.K. Freericks and D.J. Scalapino, Phys. Rev. B **49**, 6368 (1994)
  - <sup>28</sup> V. Vescoli, L. Degiorgi, H. Berger and L. Forró, Phys. Rev. Lett. **81**, 453 (1998)
  - <sup>29</sup> M. Imada, A. Fujimori and Y. Tokura, Rev. Mod. Phys. **70**, 1039 (1998)